JTTEE5 3:398-403

The "Sonarc" Process: Combining the Advantages of Arc and HVOF Spraying

H.-D. Steffens, K. Nassenstein, S. Keller, and G. Barbezat

Electric arc spraying has been successfully used for many industrial applications for more than 30 years. High-velocity oxygen fuel (HVOF) spraying is another well-established technology. Coatings produced by the HVOF process, especially carbide-containing coatings, exhibit excellent quality in terms of density and hardness. One approach to obtaining both high deposition rates and dense coatings is to combine electric arc spraying and HVOF spraying in a technique known as the "Sonarc" process. This process allows many feed combinations through the simultaneous use of wire and powder. This paper presents the development of a prototype. Examples of composite materials and structures, their properties, and potential applications are given.

1. Introduction

HIGH sonic velocity allows production of high-velocity oxygen fuel (HVOF) coatings, which are used in many industrial applications (Ref 1, 2). Arc spraying is one of the most efficient thermal spray methods for producing thick coatings and for exploiting melting power (Ref 3, 4). Alternative sonic thermal spraying processes have also been investigated and developed (Ref 5, 6).

Combining processes is another means toward the design of reinforced materials such as freestanding structures. Marantz invented the hybrid spray process known as electric arc/high-velocity oxyfuel (EA-HVOF) and first demonstrated the design and properties of metal-matrix composites (MMCs). The invention of this special spraying process combination was patented (Ref 7, 8).

Plasma-Technik of Switzerland bought the patent rights to develop an arc spraying attachment for its HVOF-System called Continuous Detonation Spraying (CDS). In cooperation with the Institute of Materials Technology at the University of Dortmund (Germany), this company is working to develop a technique known as the "Sonarc" process for industrial use.

2. Experimental Procedure

First, an arc spraying prototype to be attached to the CDS gun was designed (Fig. 1). The optimal position of the arc burning in the HVOF flame was unknown because of the influence of the pressure distribution in the gas stream (Ref 9). Therefore, the prototype device incorporated a continuously adjustable coaxial feeder to the HVOF flame, which could be altered with respect to the shock diamonds.

A thermal barrier coating (TBC) of zirconia with a Ni-Cr-Al bond layer on the copper nozzles prohibited damage from the intense heat of the HVOF flame. Moreover, the ceramic coating provided electrical isolation for the CDS gun. Axial atomizing jets cooled the contact nozzle.

The pressure of the HVOF flame caused irregular consumption of the negative and positive poled wire (Ref 10). Two calibrated electric motors pushed the wires independently, thus allowing observation of the influence of different feed rates. A direct-current (dc) electric source with a constant current characteristic supplied the melting power.

The materials and material combinations that were investigated are given in Table 1. An initial overview of the behavior of the process was gained by applying steel and nickel-chromium wires; the latter proved more difficult to process. Studies also were performed to reduce oxide formation in the supersonic flame.

In the next step, the first MMC coatings were formed. The objective was to manufacture a specific volume percentage of hard phase particles in the matrix. The coatings were metallographically prepared and investigated by optical microscopy, scanning electron microscopy (SEM), and image analysis. Hardness measurements also were performed.

3. Results and Discussion

3.1 *Process*

The Sonarc process operated at any position coaxial to the HVOF flame. There was no difference in the effect on the arc observed with respect to orientation—that is, behind, within, or in front of a shock diamond. However, splitting of the wire spray jet occurred (Fig. 2a). This effect was caused by high-frequency motion of the arc on the wire tips.

The burning position of the arc changed between the upper and the lower ends of the tips, probably because of irregularities

Table 1 Materials examined

Matrix (wire, 1.6 mm diam)	Reinforcement (powder)
X40Cr13	...
Aluminum	SiC (5-45 μm)
Ni-20Cr	SiC (5-45 μm)
	Al_2O_3 (15-45 μm)

Keywords arc spraying, composite materials, microstructure, Sonarc, spray process

H.-D. Steffens and **K. Nassenstein**, Institute of Materials Technology, Dortmund University, 44221 Dortmund, Germany; **S. Keller** and **G. Barbezat**, Plasma-Technik AG, Wohlen, Switzerland.

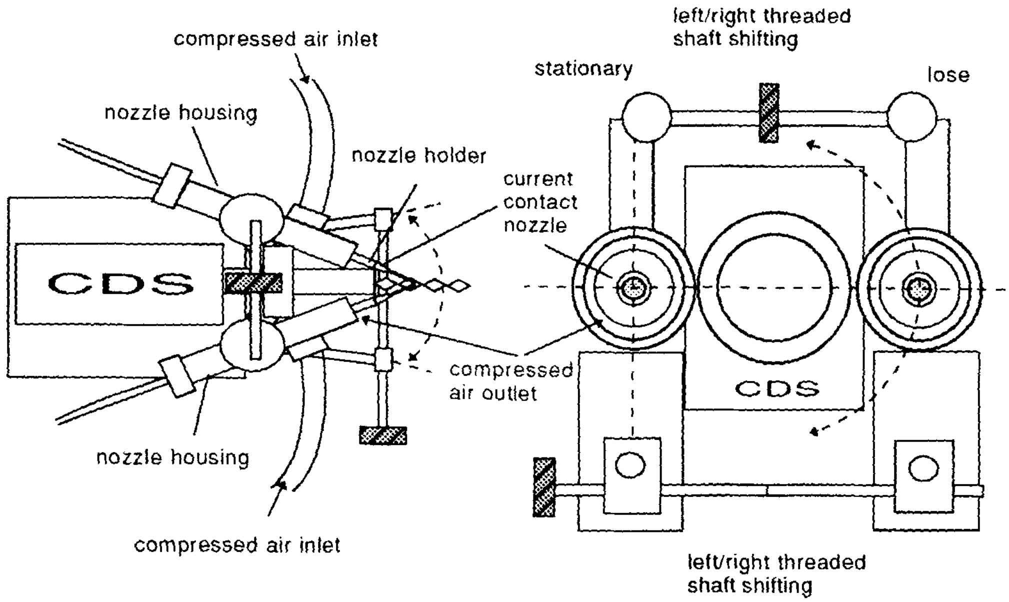

Fig. 1 Schematic of the Sonarc prototype and the various adjustments made

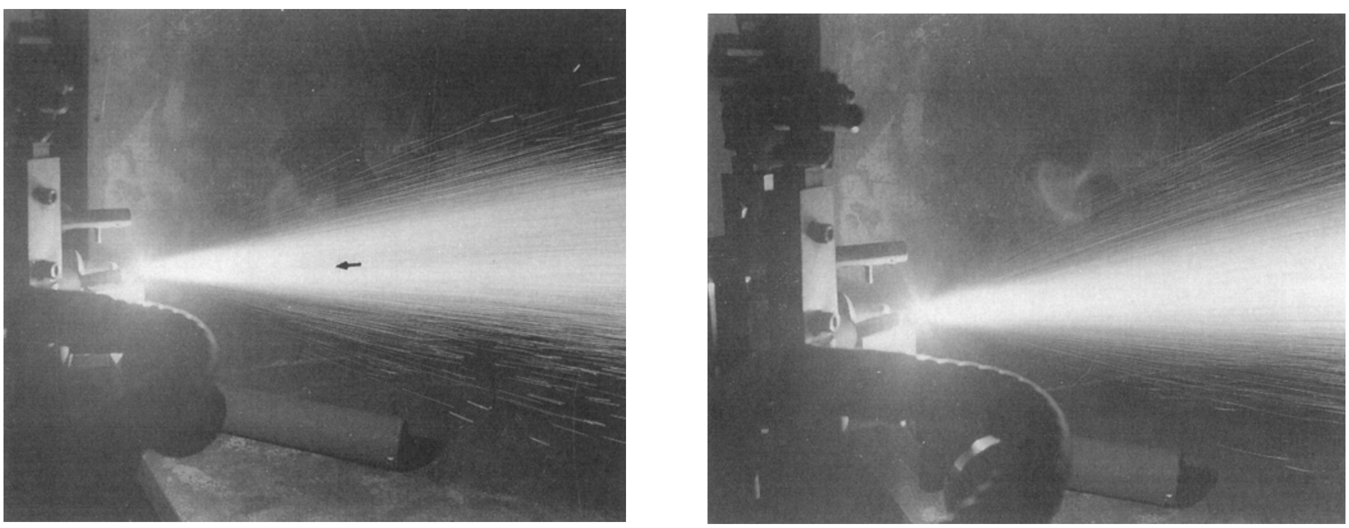

(a) (b)

Fig. 2 (a) Splitting of the spray jet (arrow) without compressed air. (b) No splitting as a consequence of applied axial compressed air

generated by the flame. Applying the axial compressed air onto the wire tips led to a constant position of the arc and a uniform spray jet (Fig. 2b). The compressed air (0.6 MPa) stabilized the arc, but the angle of the spray jet was still too wide. The spot diameter measured 80 mm at a spray distance of 350 mm. This aspect will be improved by implementing a closed-nozzle system. Consumption of both the positive and the negative wires was identical.

Abrasion and erosion caused by the wires in the nozzles constituted the largest problem. Due to the strong impulse of the gaseous mass, the nozzles became oval shaped. Furthermore, in order to prevent heat damage, the free ends of the wires were longer than is typical in conventional arc spraying. Thus, process instabilities occurred because the wire tips were not precisely guided. Contact nozzles manufactured from steel and tungsten did not improve wear resistance.

Attachment of bent nozzle holders produced different results. Nozzles bent on the inside radius (Fig. 3a) enabled better exploitation of the flame length because the arc process was positioned closer to the CDS nozzle. At the same time, however, wear of the wire nozzles increased. Nozzles bent on the outside radius exhibited less wear, but did not exploit the flame because of the geometry of the CDS gun (Fig. 3b). The problem was solved by brazing small ceramic (Al_2O_3) tubes with an outside diameter of 2.7 mm into the contact nozzles.

Another concern involved the energy consumption of the system. Although the flame possessed nearly 100 kW (420 SLPM oxygen, 55 SLPM propane) of energy, only about 0.5 kg

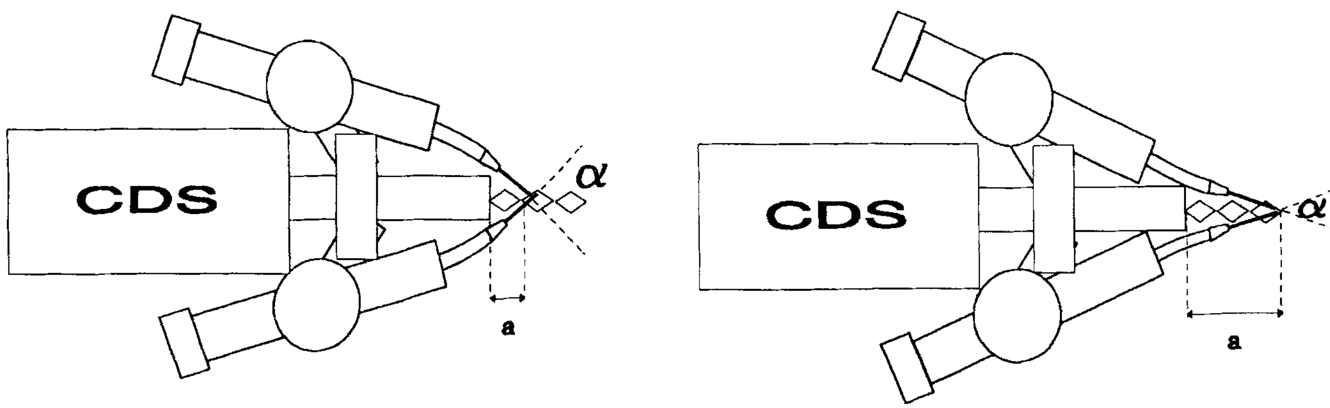

(a) (b)

Fig. 3 Bent nozzle holders. (a) Inside bending provides a narrow distance *a* of the arc to the CDS gun, requiring a wide angle α of the wire tips. (b) Outside bending fosters a close angle α, extending the distance *a*.

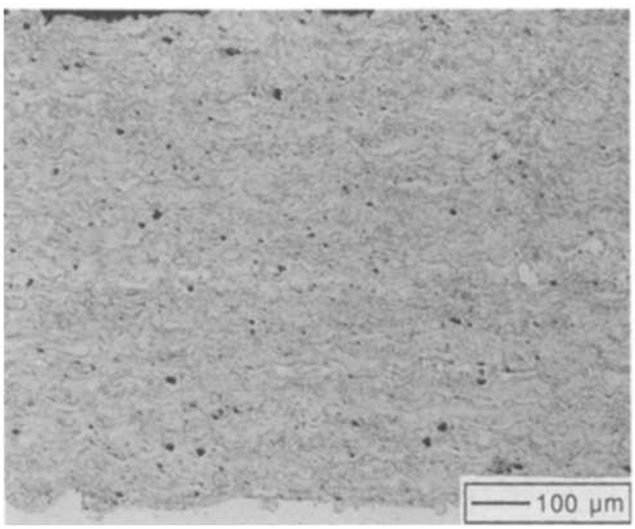

Fig. 4 Cross section of a Sonarc-sprayed X40Cr13 steel coating (420 SLPM oxygen, 55 SLPM propane, 150 A). Unetched

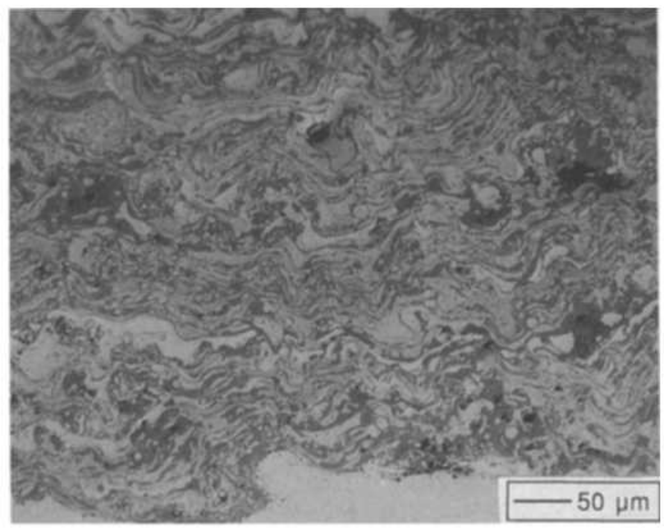

Fig. 5 Same material as in Fig. 4, showing oxides (dark gray areas)

of steel could be processed per hour without electrical power. However, the HVOF flame supplied only the atomizing gas stream and consequently the velocity. The feed rate depended on the power of the electric source. Maximum output current was 300 A, which provided a melting rate of 30 kg/h for steel. A current of 40 A formed the lower processing boundary of about 1.7 kg/h for steel. A lower wire-feed rate was impossible because of wire melting that occurred before arc ignition could be achieved. A voltage of 38 V proved to be the best value for the standing configuration (Fig. 1) in terms of process stability. The distance between the contact nozzles measured from 15 to 17 mm; at shorter distances, the CDS flame damaged the TBC coating and destroyed the nozzles.

3.2 *Coatings*

Figure 4 shows a cross section of a Sonarc-sprayed X40Cr13 coating. Four layers produced a coating thickness of 1.4 mm at a feed rate of 9 kg/h (150 A). A typical lamellar structure with a low porosity of 3% is visible, with excellent bonding to the substrate and at the interfaces of the various layers. Because of the sonic parameters (420 SLPM oxygen and 55 SLPM propane), a high amount of oxides appeared in the coating (Fig. 5, dark layers). The undesired oxides as well as nitrides cause coating properties to deteriorate and brittleness to increase, with accompanying low corrosion resistance.

Figure 6 illustrates the dependence of hardness on arc current. A decarburization process resulted in a decrease in hardness of the X40Cr13 coating. In comparison, the hardness of a coating sprayed on a mild steel with a low carbon content decreased to a lesser degree. This result agreed with another arc spraying investigation (Ref 11).

Material parameter studies were carried out to reduce the oxide content of the coating. The samples were cooled by compressed air and the spray distance optimized. The oxide content was considerably reduced by application of additional com-

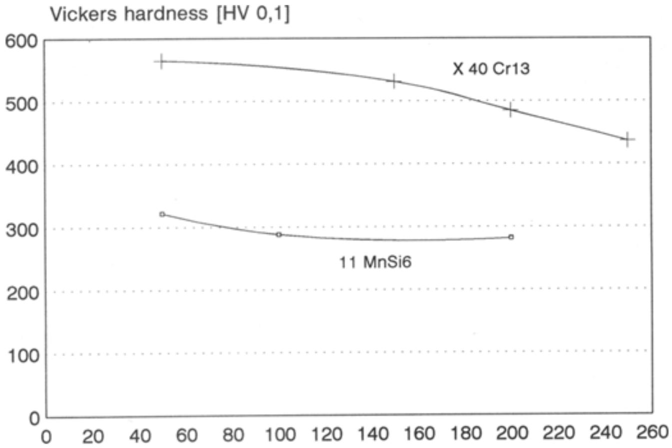

Fig. 6 Microhardness as a function of current for Sonarc-sprayed steel coatings (420 SLPM oxygen, 55 SLPM propane)

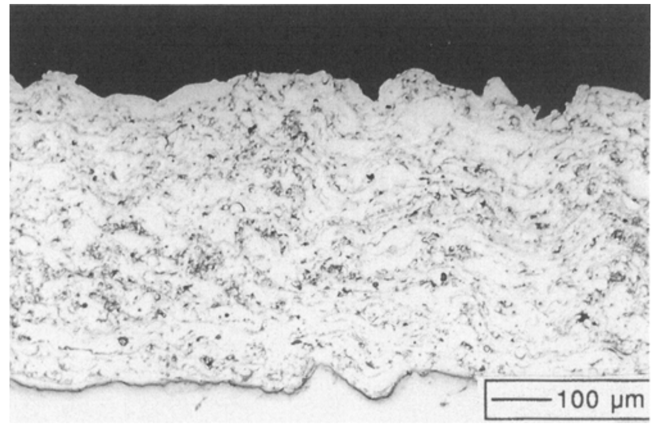

Fig. 8 Change in gas rate (270 SLPM oxygen, 90 SLPM propane) led to a dense structure containing less oxides (compare to Fig. 7b).

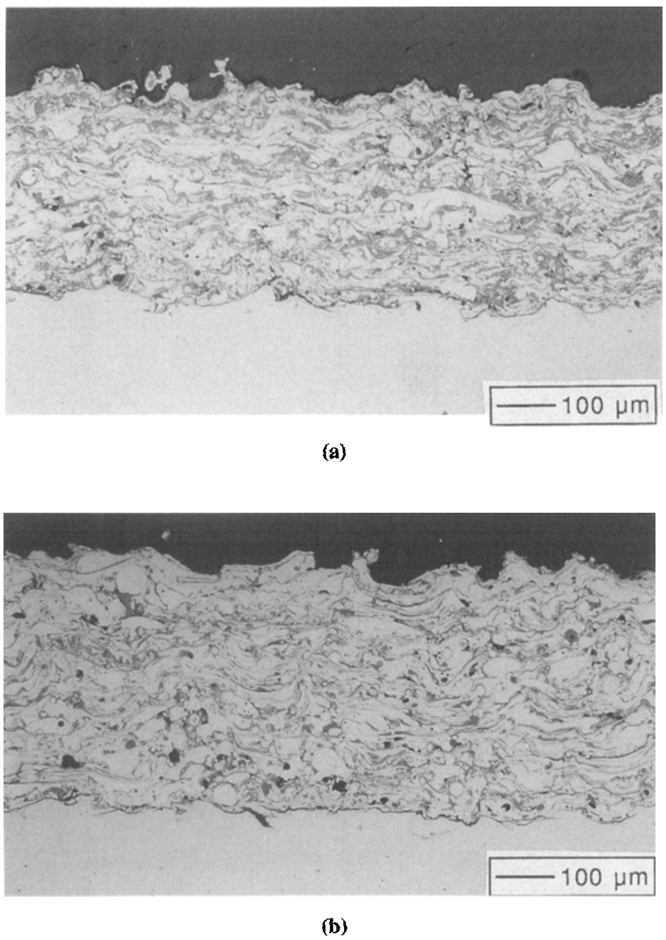

Fig. 7 Cross section through Sonarc-sprayed Ni-Cr (420 SLPM oxygen, 55 SLPM propane, 120 A, spray distance of 300 mm). (a) With axial compressed air. (b) Without compressed air

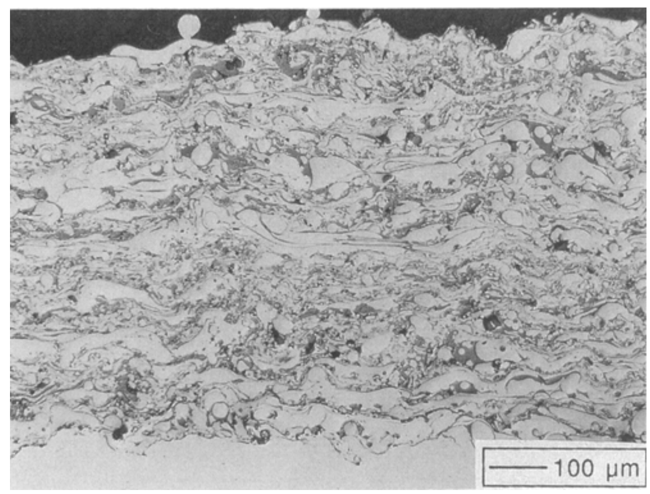

Fig. 9 Cross section through a composite coating (Ni-Cr matrix with 15 vol% SiC reinforcement). Feed rates: powder, 12 g/min; wire, 3 m/min (17 g/min)

pressed air into the spray stream. At the same time, cooling of the CDS flame occurred. Larger flattened single spray particles resulted, along with a structure of higher porosity. The number of particles that solidified in-flight increased (Fig. 7).

Changing the stoichiometry from 8:1 to 3:1 and altering the gas rate from 270 to 90 SLPM (oxygen/propane) led to the best reduction in porosity (Fig. 8). These flow parameters caused lower gas and particle velocities. Consequently, the shock diamonds disappeared and the temperature of the flame was raised.

In the next step SiC particles were fed through the CDS nozzle to obtain reinforcement of the Sonarc-sprayed Ni-Cr matrix. The optimized parameters for the Ni-Cr wire were applied to minimize oxidation. Approximately 20 vol% of reinforcement was obtained (Fig. 9).

The SiC particles reacted with both nickel and chromium as a consequence of the higher flame temperature and the reactive nature of nickel as a silicate-forming metal. The particles lost their sharp shape (Fig. 10). Scanning electron microscopy and energy-dispersive x-ray analysis supported the observations made by optical microscopy. Measurement of the SiC parti-

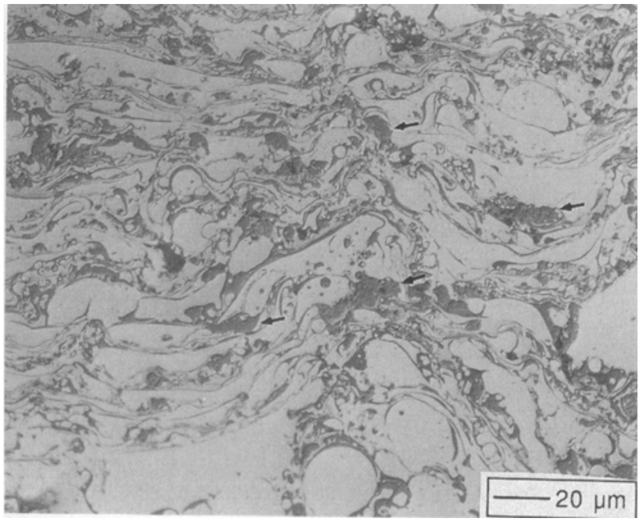

Fig. 10 Optical micrograph of SiC-reinforced Ni-Cr. Particles show reaction at boundary with the Ni-Cr matrix.

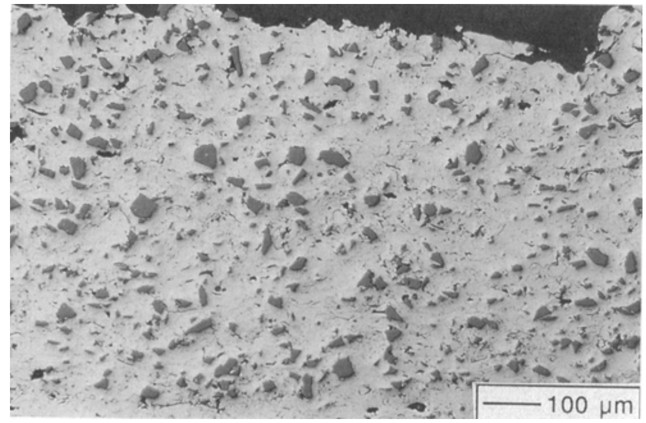

Fig. 12 SiC reinforcement (20 vol%) in an aluminum matrix. Feed rates: powder, 13 g/min; wire, 9 m/min (54 g/min)

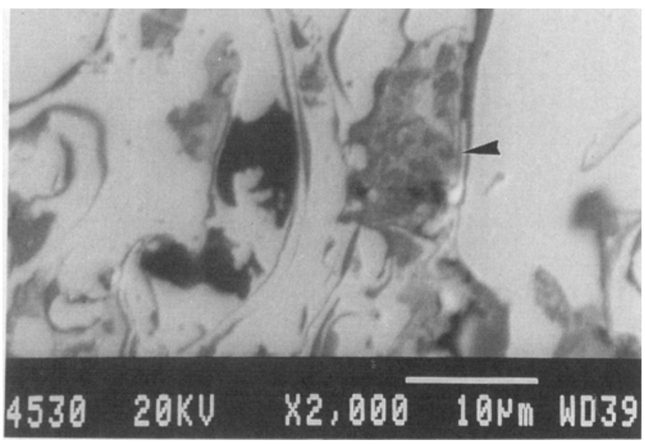

Fig. 11 SEM micrograph of an Al_2O_3 particle (arrow), showing total reaction with the Ni-Cr matrix

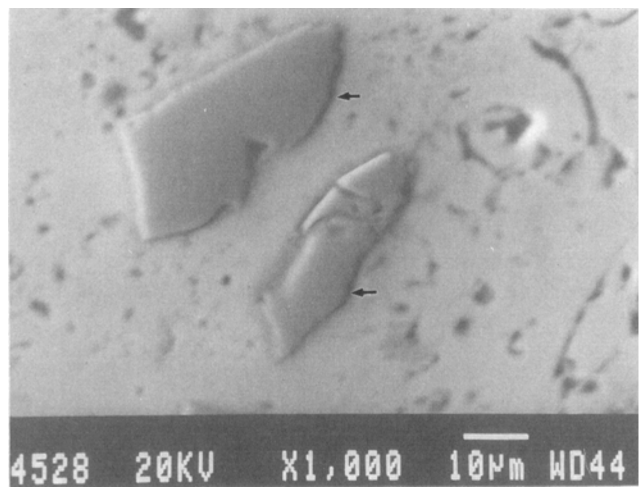

Fig. 13 SEM micrograph of an SiC particle (arrow), showing no reaction with the aluminum matrix

cle boundaries confirmed a concentration of chromium and nickelelements.

The Al_2O_3 particles experienced the same effect (Fig. 11). However, whereas the seed of the SiC particles in the Ni-Cr matrix retained their composition, the Al_2O_3 particles reacted totally with the matrix by taking up nickel and chromium.

Reinforcement of aluminum with SiC particles produced the best results in terms of structure and distribution. Figure 12 reveals an SiC particle content of approximately 15 vol%. The particles were homogeneously distributed and did not react with the matrix material. Moreover, deposition rates of 4 kg/h of SiC/Al were achieved without reaching the maximum limit of 12 kg/h. Figure 13 verifies the good incorporation of the SiC particles; the sharp features of the particles were preserved as a consequence of no reaction with the aluminum matrix.

Figure 14 presents the results of microhardness measurements. Reinforcement resulted in increased coating hardness.

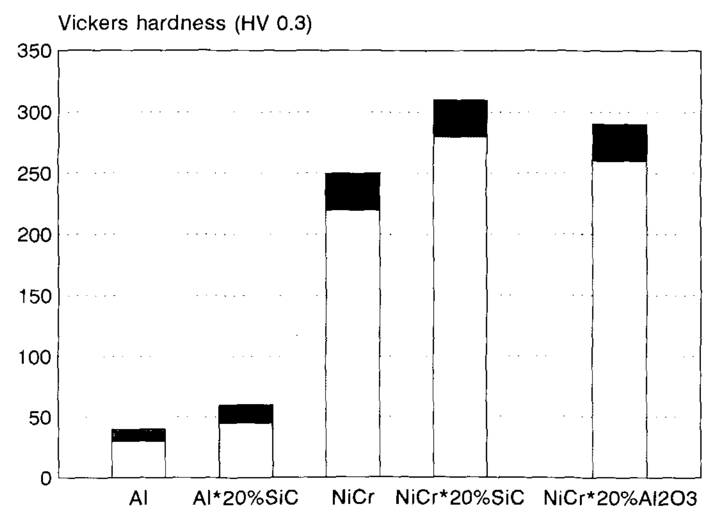

Fig. 14 Microhardness of various Sonarc-sprayed composite materials compared with nonreinforced material

Compared to conventional arc-sprayed coatings, 20 vol% of SiC raised the hardness of aluminum and Ni-20Cr coatings by about 30%. Feeding 20 vol% of Al_2O_3 into Ni-20Cr increased hardness by 20%. Other research work is under way to increase the volume percentage of reinforcement and to determine such coating parameters as wear resistance, corrosion resistance, and mechanical properties.

4. Conclusions

A spray process that combines HVOF and electric arc spraying has been developed. The Sonarc process operates at any position coaxial to the HVOF flame. The power of the flame did not raise the melting rate, but it did improve the structure of the arc-sprayed coatings in terms of porosity and bonding to the substrate and between the sprayed layers. At the same time, reducing the flame parameters decreased the oxide content in the arc-sprayed coatings.

The Sonarc process was suitable for producing composite materials with homogeneously distributed reinforcement that increased coating hardness. The particle amount was calculated and controlled by the relation between wire and powder feed.

References

1. P. Sahoo, High Performance Wear Coatings—The Quest Continues, *Powder Metall. Int.*, Vol 2, 1993, p 73-78
2. L.N. Moskowitz, Application of HVOF Thermal Spraying to Solve Corrosion Problems in the Petroleum Industry—An Industrial Note, *J. Thermal Spray Technol.*, Vol 2 (No. 1), 1993, p 21-29
3. K.D. Borbeck and A.R. Nicoli, The Design and Development of Plasma Torches for the Industrial Fabrication of Surface Protective Layers, *Proc. ATTAC 88*, The Welding Institute, 1988
4. D.R. Marantz, State of the Art Spray Technology, *Thermal Spray Research and Applications*, T.F. Bernecki, Ed., ASM International, 1991
5. J. Browning, Further Developments of the High Velocity Impact Fuel-(HVIF) Process, *Proc. 2nd Conf. Thermal Spray*, Aachen, Germany, Deutscher Verband Für Schweißtechnik (DVS), Vol. 152, 1993, p 52-54
6. I. Karp et al., Electric Arc Spraying in Supersonic Stream, *Proc. 5th Natl. Thermal Spray Conf.*, ASM International, 1993, p 185-190
7. D.R. Marantz, U.S. Patent 5,206,059, April 1993
8. R. Tiwari, H. Herman, K.A. Kowalsky, and D.R. Marantz, Thermal Spray Forming of Particulate Composites, *Thermal Spray Research and Applications*, T.F. Bernecki, Ed., ASM International, 1991, p 393-399
9. M.L. Thorpe and H.J. Richter, A Pragmatic Analysis and Comparison of the HVOF-Process, *Thermal Spray: International Advances in Coatings Technology*, C.C. Berndt, Ed., ASM International, 1992, p 137-147
10. M. Wewel, "Contribution to Arc Spraying in Low Pressure Atmosphere," doctoral thesis, Verein Deutscher Ingenieure (VDI), 1992, p 34 (in German)
11. M. Nakagawa et al., Development of Mass Production Technology of Arc Spraying for Automotive Engine Aluminum Alloy Valve Lifters, *Thermal Spray Research and Applications*, T.F. Bernecki, Ed., ASM International, 1991, p 457-464